REGOLITH PROPERTIES AT LUNAR SWIRLS FROM HIGH-RESOLUTION PHOTOMETRIC OBSERVATIONS. Brett W. Denevi[1], Hiroyuki Sato[2,3], Anna C. Martin[1], Aaron K. Boyd[3], Bruce W. Hapke[4], Mallory J. Kinczyk[5], and Mark S. Robinson[3], [1]Johns Hopkins University Applied Physics Laboratory, Laurel, MD 20723, USA. [2]Japan Aerospace Exploration Agency, 3-1-1 Yoshinodai, Tyuo-ku, Sagamihara, Kanagawa, Japan. [3]Arizona State University, Tempe, AZ 85287, USA. [4]University of Pittsburgh, Pittsburgh, PA 15260, USA. [5]North Carolina State University, Raleigh, NC 27695, USA.

Introduction: Lunar swirls are sinuous high-reflectance surface features (Fig. 1) [e.g., 1,2] co-located with crustal magnetic anomalies [3]. Various models for their formation have been proposed, including reduced or altered space weathering due to solar wind shielding [e.g., 3–7], scouring of the surface by cometary impacts to expose fresh material and/or compact the regolith [8,9], and sorting of electrostatically levitated soil [10,11]. Discriminating between these formation models will provide new information about the nature of lunar space weathering, magnetic anomalies, and lunar surface processes.

In this work we examine the photometric properties of swirls as one avenue through which we can better understand their nature. Past studies have suggested that the regolith at lunar swirls is more forward scattering (i.e., more reflective at large phase angles) than the ejecta of fresh craters [8,12–14]. These photometric differences have been interpreted as indicating that swirl regolith is dissimilar from both typical immature and mature regolith, specifically that it is anomalous in terms of its textural properties (e.g., differences in mm-scale structure or depletion of fine particles) [12–15]. Here we present comprehensive photometric observations from the Lunar Reconnaissance Orbiter Camera (LROC) Narrow Angle Camera (NAC) and the final results of radiative transfer modeling to aid in assessing these hypotheses for swirl formation.

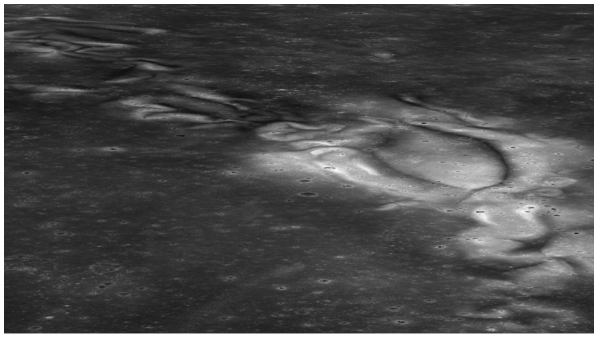

Fig. 1. High-phase (103°) LROC NAC image (M1236922564) from the photometric sequence of Reiner Gamma. Each point in Fig. 2 represents data collected from a single image for swirl regolith (high-reflectance region), non-swirl regolith (lower reflectance regolith nearby), and fresh impact craters within the high-reflectance region of the swirl, and outside of the swirl.

Data and Methods: A series of LROC NAC images was collected for three swirl sites: Reiner Gamma (82 images), Mare Ingenii (48 images), and the Firsov highlands (48 images). These images for each of the three sites were targeted to span the broadest possible range of phase angles (<6° to >100° phase). For each site, a NAC digital terrain model (DTM) was created at a pixel scale of 5 meters using the SOCET SET Toolkit [16]. The NAC images were then orthorectified and controlled to the DTM [17] so that incidence and emission angles could be calculated taking into account local slopes. Regions of interest were selected to include portions of each swirl that stepped through its full range of reflectance, neighboring non-swirl regolith, and the ejecta of fresh impact craters that formed both within the high-reflectance portions of swirls and in the neighboring non-swirl regolith. For each region of interest, the average reflectance, phase, incidence, and emission angles were extracted from all overlapping images (e.g., Fig. 2).

Hapke radiative transfer modeling based on the methodology of Sato and co-workers [18] was employed to compare the photometric properties of the regolith within swirls, non-swirl regions, and fresh impact crater ejecta. This modeling gives estimates of parameters such as single-scattering albedo (*w*, the probability of a photon being scattered by a regolith particle) and *b* and *c* (the forward and backward scattering portions of

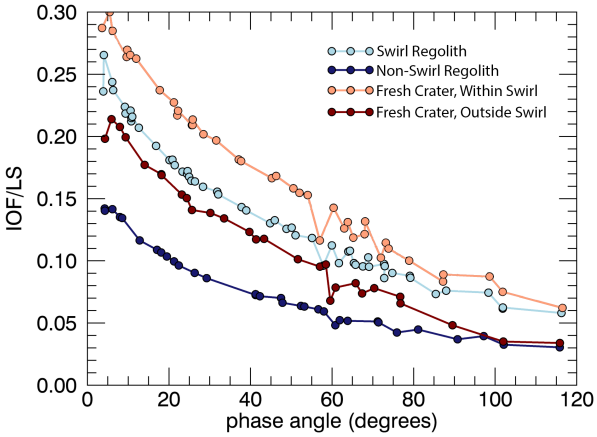

Fig. 2. LROC NAC photometry data for example regions of interest at Reiner Gamma. Reflectance (IOF) is normalized to the Lommel-Seeliger (LS) function.

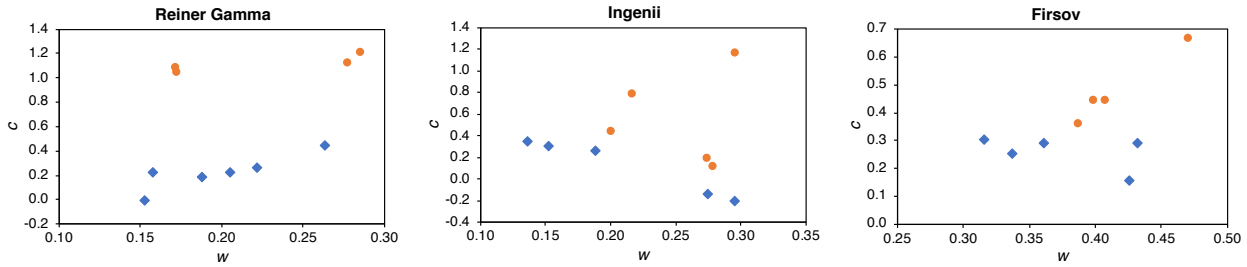

Fig. 3. Hapke model results for single scattering albedo (*w*; higher values indicate a higher reflectance surface) and backscattering (*c*; higher values indicate a more backscattering surface) for the Reiner Gamma, Ingenii, and Firsov locations. Swirl and non-swirl regolith (blue diamonds) and the ejecta of fresh impact craters located inside and outside of swirls (orange circles) are shown. Regardless of their location, fresh crater ejecta is more highly backscattering than swirl and non-swirl regolith.

the double-lobed Henyey–Greenstein single particle phase function) and provides a means for a quantitative comparison of the physical properties of the regolith in different regions of interest at each swirl. Because we optimized the range of phase, incidence, and emission angles used in our model to each individual site, the model results for regions of interest can be compared within a single swirl site, but not across sites.

Results: The LROC NAC photometric data sets confirm that swirls and fresh impact craters (located both inside and outside of swirls) typically have different photometric properties (Fig. 2, 3). While both are generally still in the backscattering regime (positive values of *c*), swirls are more forward scattering than fresh impact ejecta (lower *c* values, Fig. 3). However, while swirls have a higher albedo than mature regolith, their backscattering nature is comparable (similar *c* values for swirl and non-swirl regolith, Fig. 3).

Fresh impact ejecta displays a wider range of photometric properties. Some fresh ejecta that is substantially higher in reflectance than nearby regolith when viewed at low phase angles is also higher than surroundings when viewed at high phase angles (greater than ~80–90°), albeit with reduced contrast. However other fresh craters show reversals in contrast, where at high phase angles they are lower in reflectance than nearby regolith. At Reiner Gamma, craters that are highly backscattering are typically blocky when resolved in NAC images. The heterogeneity in photometric properties of ejecta is likely related to target properties and crater age.

Discussion: Resolved photometric parameter maps of the Moon revealed that fresh highland impact crater ejecta is among the most backscattering of all lunar materials [18]. This is likely due to differences in sub-pixel scale roughness [19,20] or the presence of optically thick clasts [18], and suggests that fresh materials exposed by impacts have distinct photometric properties due to physical properties that result from the impact process, rather than their immature nature alone. This is supported by the observation of blocks at highly backscattering craters in the Reiner Gamma region. The regolith in this area is thinner than in Mare Ingenii or the Firsov highlands, thus blocks are more common in impact ejecta. Based on their high degree of backscattering (high *c* values), we suspect that even when blocks are not resolved, there are larger, optically thick particles at all of the fresh impact craters that we examined, or that the regolith has been roughened by the impact process.

Our photometric data sets and modeling results suggest that swirls have scattering properties similar to non-swirl regolith. At least in terms of their photometric properties, the regolith at lunar swirls is entirely typical. This observation suggests swirl formation does not require a recent cometary impact event or another process that would alter the regolith structure, consistent with results from thermal infrared observations [7]. An atypical space weathering environment due to solar wind shielding remains a compelling hypothesis for the cause of the high reflectance of lunar swirls.

References: [1] Strom R.G. and Whitaker E.A. (1969) *Apollo 10 Photography and Visual Observations, NASA SP-232*, 20–24. [2] El-Baz F. (1972) *Apollo 16 Prelim. Sci. Rep., NASA SP-315*, 29-93–29-97. [3] Hood L.L. and Schubert G. (1980) *Science*, *208*, 49–51. [4] Hood L.L. and Williams C.R. (1989) *LPSC 19*, 99–113. [5] Blewett D.T. et al. (2011) *JGR*, *116*, doi:10.1029/2010JE004656. [6] Kramer G.Y. et al. (2011) *JGR*, *116*, E04008. [7] Glotch T.D. et al. (2015) *Nature Comm.*, *6*, 6189. [8] Schultz P.H. and Srnka L.J. (1980) *Nature*, *284*, 22–26. [9] Bruck Syal M. and Schultz P.H. (2015) *Icarus*, *257*, 194–206. [10] Garrick-Bethell I. et al. (2011) *Icarus*, *212*, 480–492. [11] Pieters C.M. et al. (2014) *LPSC 45*, Abs. 1408. [12] Kaydash V. et al. (2009) *Icarus*, *202*, 393–413. [13] Pinet P.C. et al. (2000) *JGR*, *105*, 9457–9475. [14] Kreslavsky M.A. and Shkuratov Y.G. (2003) *JGR*, *108*, 5015. [15] Starukhina L.V. and Shkuratov Y.G. (2004) *Icarus*, *167*, 136–147. [16] Miller S.B. and Walker A.S. (1993) *ACSM/ASPRS Ann. Conv.*, *3*, 256–263. [17] Martin A. C. et al. (2018) *LPSC 49*, Abs. 1621. [18] Sato H. et al. (2014) *JGRP 119*, 1775–1805. [19] Shkuratov Y. et al. (2011) *PSS*, *59*, 1326–1371. [20] Kaydash V. et al. (2014) *Icarus*, *231*, 22–33.